Diffusion-Map: A Novel Visualizing Biomarker for Diffusion Tensor Imaging of Human Brain White Matter

Mohammad Hadi Aarabi and Hamid Saligheh Rad

Abstract Rich information about brain tissue microstructure and composition is yielded by MRI-based measurement of the local diffusion tensor (DT) of water molecules in neural fibers, whose axons are running in myelinated fiber tracts. Diffusion tensor imaging (DTI) possesses high-dimensional and complex structure, so that detecting available pattern information and its analysis based on conventional linear statistics and classification methods become inefficient. Classification, segmentation, compression or visualization of the data could be facilitated through dimension reduction. The previously proposed methods mostly rely on complex low dimensional manifold embedding of the high-dimensional space, which are not able to deal with complex and high dimensional data. The purpose of this paper is to propose a new method for meaningful visualization of brain white matter using diffusion tensor data to map the six-dimensional tensor to a three dimensional space, employing Markov random walk and diffusion distance algorithms, leading to a new distance-preserving map for the DTI data with lower dimension and higher throughput information.

1 Introduction

To gain a better insight into the disease effects on brain anatomy and physiology, a systematic pattern of anatomy must be detected in anatomical imaging of the brain. Diffusion tensor imaging (DTI) is a promising method, which yields fundamental information of the brain tissue microstructure and composition by means of magnetic resonance imaging (MRI)-based measurement of local diffusion tensor (DT) of water molecules in human brain [1]. In particular, DTI is used to characterize and map the three dimensional (3D) diffusion of water, as a function of spatial location and generate 3D quantitative maps like mean-diffusivity (MD) or fractional-anisotropy (FA), obtained from dominant orientation of water diffusion

M.H. Aarabi (✉) • H. Saligheh Rad
Quantitative MR Imaging and Spectroscopy Group, Research Center for Molecular and Cellular Imaging, Tehran University of Medical Sciences, Tehran, Iran
e-mail: m-aarabi@razi.tums.ac.ir; h-salighehrad@tums.ac.ir

L. O'Donnell et al. (eds.), *Computational Diffusion MRI*, Mathematics and Visualization, DOI 10.1007/978-3-319-11182-7_7

for each voxel in the image. Brain regions, such as cortical and subcortical gray matter and cerebrospinal fluid, have a vast isotropic diffusivity due to the lack of constraining process of diffusion by axons, running in myelinated fiber tracts [6]. The diffusion tensor can be used for characterizing magnitude, degree of anisotropy and orientation of directional diffusion. Therefore, mapping diffusion anisotropy and principal diffusion directions is one of the best ways to estimate white matter connectivity patterns in the brain obtained from white matter tractography. This could result in voxel-wise and tensor-wise analysis of diffusivity and anisotropic change in the white matter, which enables neuroscientists to chart the complex network of neural fiber tracts in the human brain. DTI possesses high dimension and complex structure, so that, detecting available pattern information and its analysis are mainly based on conventional linear statistics and classification methods become inefficient. In order to facilitate classification, segmentation, compression or visualization of the data, alleviating the undesirable properties of high-dimensional spaces, i.e. dimensionality reduction, is far-reaching. Dimensionality reduction is based on finding valid structures and geometric characterization of high dimensional data, to be realized with several techniques, which are categorized into linear and nonlinear methods. Linear methods are based on classic approaches, such as principal component analysis (PCA) and multi-dimensional scaling (MDS) [12]. Although they guarantee acquisition of real data structures lying on or near a linear subspace of high dimensional input space, they cannot deal with complex nonlinear data. This has led to development of nonlinear methods, such as Kernel PCA [9], and Isomap and diffusion-map (DM) techniques for biological data with highly nonlinear manifolds [2,7,8,10–13]. This paper seeks to address a technique for multiple valued DTI data visualization, based on images with pixels, sampled from underlying manifold, e.g. every single pixel may consist of a high dimensional vector as a positive semi-definite tensor in a DT-MRI acquisition. Diffusion map (DM) represents a dataset via a weighted graph of corresponding points to vertices and edges, in which, the spectral properties of the graph Laplacian would be used to map six-dimensional data to a 3D representation. Diffusion distance is applied by using a specific value, which is obtained for the proximity of each data point, performing the random walk for a number of time steps. Thus, pairwise diffusion distances in the low-dimensional representation of the data is maintained [4,5]. Differences between DT-MRI pixels are mainly evaluated using a diffusion distance metric with regard to rank 3, second-order positive semi-definite DTs, while the difference between DT pixels is approximated by DM. In this article, we evaluated case studies of high-dimensional phantom data, as well as normal clinical brain DT-MRI.

2 Method

To represent the underlying DTI data, high dimensional DT-MRI data are used. As long as the pixel dimensionality is greater than 3D space, dimensionality reduction must be employed in order to represent the low dimensional image pixels. To

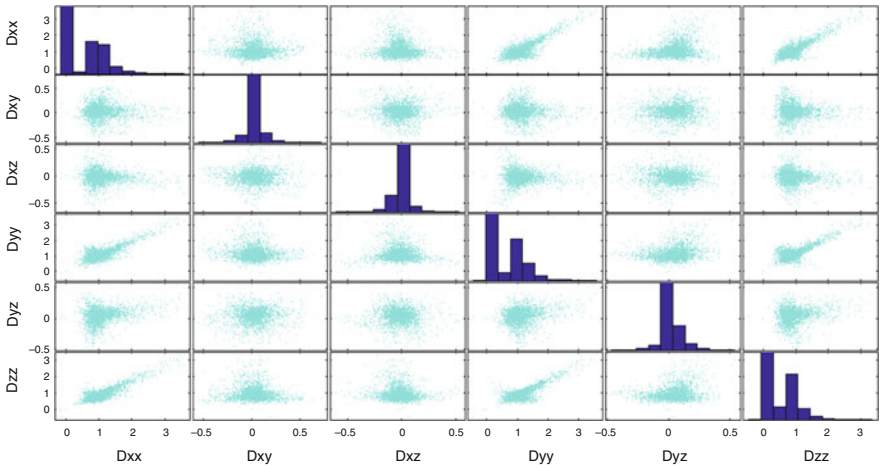

Fig. 1 Distribution of multi-dimensional DT-MR data

achieve this intention, pixel dissimilarities must be measured and pixels must be mapped to perceptually meaningful colors [3, 13]. It is assumed that high dimensional pixel values are sampled from underlying manifold acquired with distance metric. The manifolds are either learned using manifold learning techniques (e.g. DM), derived analytically or by approximation. Diffusion distance between two corresponding points on the manifold are the measured differences between any two high dimensional pixels. Similarities between DT pixels are evaluated by diffusion metric that scales the rank 3 manifold of DT pixels. DTs are symmetric 3×3 matrices, or second-order rank 3 diffusion tensors, with six unique elements. Furthermore, DTs must be positive semi-definite (PSD), in that six unique elements are defined in Diffusion tensors which are symmetric 3×3 matrices, i.e. $f(x) : x \in R^3 \rightarrow R^6$. An example of data distribution of a real data is shown in Fig. 1.

2.1 Dissimilarity Between High Dimensional Diffusion Tensor Imaging Data

Measuring dissimilarities between observations is an important step in handling high dimensional data. As far as the DT-MRI goes, estimation of DM and dissimilarity metrics are needed for the manifold learning structures, assuming $x^1, x^2, \ldots, x^k \in M$, M is the manifold embedded in R^3.

2.2 Implementation of Diffusion Map Algorithm in DT-MRI

The implemented algorithm proposed for DT-MRI of human brain is outlined in six steps as follows:

1. Constructing the similarity matrix, W, of the graph; the entries of W are the weights along the edges connecting corresponding nodes i and j, to be determined by the heat kernel as follows [13]:

$$W_{ij} = exp(-\frac{\|x_i - x_j\|^2}{\epsilon}) \tag{1}$$

where W is PSD and $\|.\|$ is the Euclidean norm. One should note that $W \in R^{k\times k}$ is a symmetric matrix. In the DM algorithm, the choice of the parameter ϵ is very important. Lafon in chose ϵ to be in the order of the average smallest non-zero value of $\|x_i - x_j\|^2$, that is:

$$\epsilon = \frac{1}{k}\sum_{i=1}^{k} min\|x_i - x_j\|^2; x_i \neq x_j \tag{2}$$

2. Formulating $k \times k$ normalization matrix of D; diagonal entries of D are row or column sum of W [11]:

$$D_{ii} = \sum_{i=1}^{n} W_{ij}, i \in 1, \ldots, n \tag{3}$$

The W matrix is then normalized as

$$P = D^{-1}W \tag{4}$$

Since DMs originate from dynamical systems theory, the resulting matrix P is considered to be a Markov matrix that defines the forward transition probability matrix of a data point.

3. Find the eigenvalues of P; the conjugate matrix of P is calculated as below:

$$\tilde{P} = D^{-\frac{1}{2}}WD^{\frac{1}{2}} \tag{5}$$

This so-called normalized graph Laplacian preserves the eigenvalues.

4. Singular value decomposition (SVD) of $\tilde{P}$ to be calculated by:

$$\tilde{P} = U\Lambda U^* \tag{6}$$

yielding the eigenvalues

$$\Lambda = diag([\lambda_1, \lambda_2, \ldots, \lambda_n]) \tag{7}$$

and eigenvectors in matrix

$$U = [u_1, u_2, \ldots, u_n] \tag{8}$$

[2]

5. Computing eigenvectors of $\tilde{P}$; one notes that eigenvalues of P and $\tilde{P}$ stay the same

$$V = D^{\frac{1}{2}}U \tag{9}$$

6. Creating low-dimensional coordinates in the embedded space Ψ using Λ and V, as follows:

$$\Psi = V\Lambda \tag{10}$$

Now, for each n-dimensional point x_i, there is a corresponding d-dimensional coordinate, where d < n. The coordinates for a single point can be expressed as:

$$\Psi_d : x_i \rightarrow [\lambda_1 v_1, \lambda_2 v_2, \ldots, \lambda_{d+1} v_{d+1}]. \tag{11}$$

Finally, diffusion map (DM) is defined as:

$$DM = \frac{[\lambda_1 v_1 + \lambda_2 v_2 + \lambda_3 v_3]}{3}. \tag{12}$$

An overview of all these steps is shown in Fig. 2.

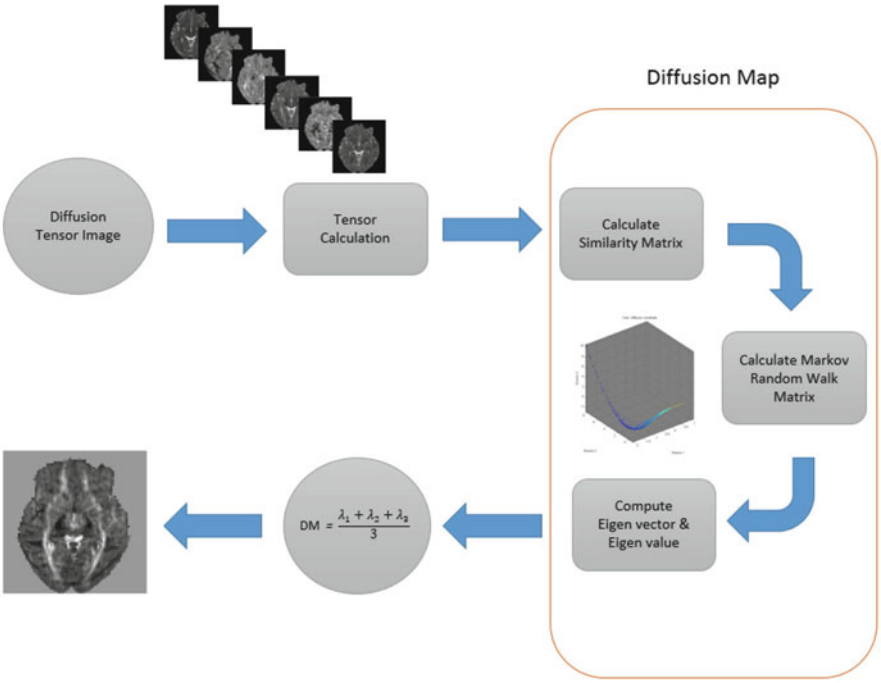

Fig. 2 Overview of proposed method

3 DT-MR Data

The idea of generating simulated MR images for this work are adopted from. The fibers were constructed based on streamline algorithm in ExploreDTI software [13]. The six tensor elements were calculated using linear fitting methods. MR acquisition on real data was performed on four normal subjects on a 1.5T clinical scanner MAGNETOM Avanto (Siemens Medical Solution, Erlangen, Germany) equipped with a maximum gradient strength of 40 mT/m and a slew rate of 200 mT/m/s. DT images were obtained with a single-shot echo-planar sequence with TR = 4,900 ms, TE = 85 ms, *b-value*= 1,000 s/mm^2, FOV = 230 mm, matrix size = 76×76, slice thickness = 3 mm, number of directions = 30, and NEX = 1.

4 Results and Discussion

4.1 Simulated MR Images

The implemented DM method was compared with fractional anisotropy (FA) and mean diffusivity (MD) maps (as shown in Fig. 3) on the simulated data. We quantitatively evaluated the image energy resulting from each method as indicated in Table 1, in terms of entropy, contrast, and correlation, which are defined as follows:

1. Entropy is a statistical measure of the randomness of data, representing the texture of the image:

$$Entropy = -\sum_{a}^{b} Plog_2 P \tag{13}$$

2. Contrast is a measure of intensity contrast, calculated between a pixel and its neighbor on the whole image:

$$Contrast = \sum_{i}^{j} |i - j|^2 p(i, j) \tag{14}$$

3. Correlation returns the amount of similarity between a pixel and its neighbor over the whole image:

$$Correlation = \sum_{i,j} \frac{(i - \mu i)(j - \mu j)p(i, j)}{\sigma_i \sigma_j} \tag{15}$$

The higher value of entropy and contrast, and lower correlation represent higher energy and more heterogeneity among the provided information. It can be inferred from Fig. 3 and Table 1 that DM technique yields higher amount of entropy and

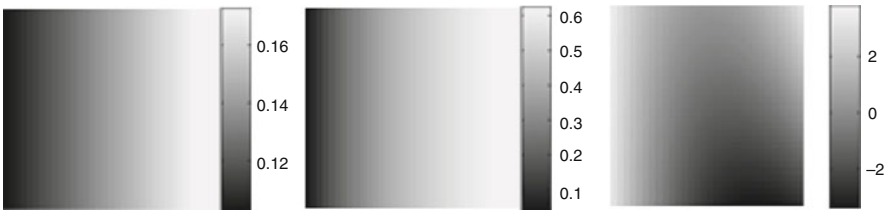

Fig. 3 Simulated data obtained using, mean diffusivity (MD) and fractional anisotropy (FA) maps in comparison with the proposed diffusion map (DM)

Table 1 Evaluation of the proposed diffusion map (DM), in comparison with mean diffusivity (MD) and fractional anisotropy (FA) maps, in terms of entropy, contrast, and correlation

Map	Entropy	Contrast	Correlation
DM	5.7014	0.2419	0.9690
MD	4.1800	0.2333	0.9827
FA	4.9542	0.2333	0.9827

Table 2 The amount of similarity between FA and DM

Correlation coefficient r	−0.5392
Significance level	P<0.0001
95 % confidence interval for r	−0.5573 to −0.5207

Table 3 The amount of similarity between MD and DM

Correlation coefficient r	0.5967
Significance level	P<0.0001
95 % confidence interval for r	0.5798–0.6130

contrast, and lower correlation value in comparison with FA and MD maps, meaning that it extracts more information from a DT-MR image.

4.2 Real MR Images

In Tables 2 and 3, the amount of similarity between DM and FA, MD are calculated in terms of correlation coefficient and the significance of this correlation is assessed by p-value. It can be observed that DM has high correlation with both FA and MD with a significant level ($p<0.0001$). This means that DM could contain essential information from both FA and MD, providing better visualization of the information in DT-MRI. Figure 4 illustrates the results of applying the proposed DM technique and calculated FA and MD maps on the real data. It is apparent that DM map contains more information than T1-weighted image, MD and FA maps. This suggests that DM could be reliably employed for further statistical analysis of human brain. Figure 4 demonstrates the values of DM, MD and FA on the region of interest (ROI), located on the hippocampus region in the coronal view of the T1-weighted image. For convenient analysis, MD values are multiplied by 1,000 to bring it into the same scale as FA and DM. The pixel intensity versus pixel number plot shows that when MD is high, FA and DM have reverse signs and when

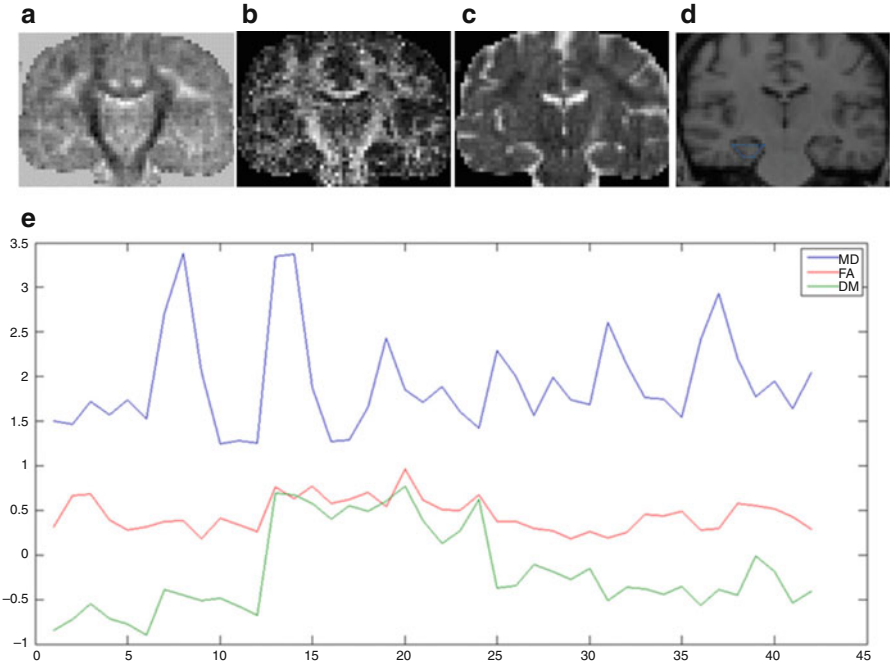

Fig. 4 The results on real data (**a**) T1-weighted image in a coronal view, with a region-of-interest (ROI) located on the hippocampal region; (**b**) the corresponding MD map; (**c**) fractional anisotropy (FA) map; (**d**) the proposed diffusion map (DM); and (**e**) the values of MD, FA, and DM on the selected ROI in part (**a**). The MD values are multiplied by 1,000 to be in the same scale as FA and DM

MD is low, their relationship is held with the similar sign. This suggests that DM has mutual information from both FA and MD, recommending a new visualization technique consisting of the necessary information of FA and MD, which could be used as a proper substitute for clinical applications. The visualization of DM, MD and FA are compared on several slices of a normal subject in axial, coronal and sagittal views in Figs. 5, 6, and 7.

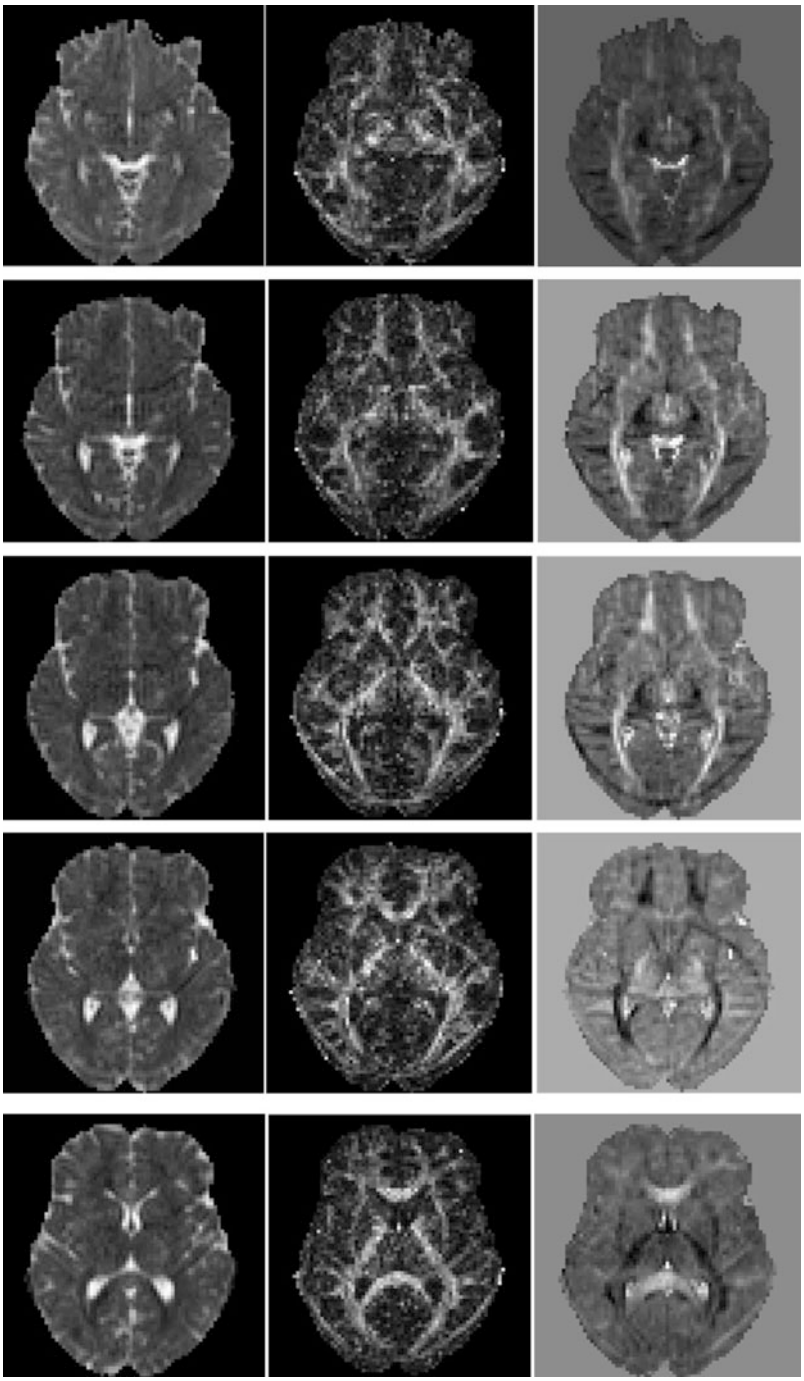

Fig. 5 Axial view of the results on real data: (*left column*) MD map, (*middle column*) FA map, and (*right column*) proposed diffusion map (DM)

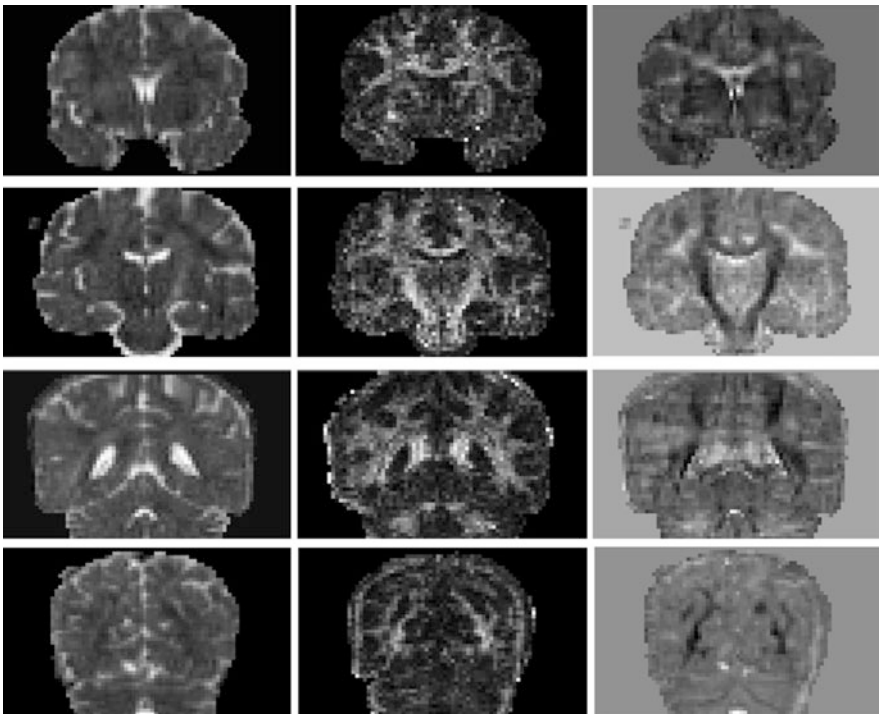

Fig. 6 Coronal view of the results on real data: (*left column*) MD map, (*middle column*) FA map, and (*right column*) proposed diffusion map (DM)

5 Conclusion

This study set out to propose a method for visualization of diffusion tensor (DT)-MRI as a robust method to noise, preserving distance in nonlinear data, while keeping low-dimensional space. The proposed analysis suggests that the diffusion map (DM) dimensionality reduction improves white matter segmentation and visualization, particularly in the low-SNR regimen of DT-MRI, while it stays an active research problem. Due to the wide range of research and clinical applications of DT-MRI, we hope that the proposed method will broaden new horizons for exploring the full richness of DTI to realize ways, in which such measurements are affected by pathologies and treatments. Manifold learning problems involve vector bundle on graphs providing the demand for vector diffusion mapping. Since vector diffusion mapping is an extended form of diffusion mapping, their properties and convergence behavior are similar. Besides, because the idea of vector diffusion mapping is a natural extended form of graph Laplacian operator combined with diffusion mapping on graphs, in the future, we are going to investigate the issues of smoothing and interpolation, as well as clustering of components of DTI datasets, leading to successful fiber clustering. In this work, it was indicated that DM could

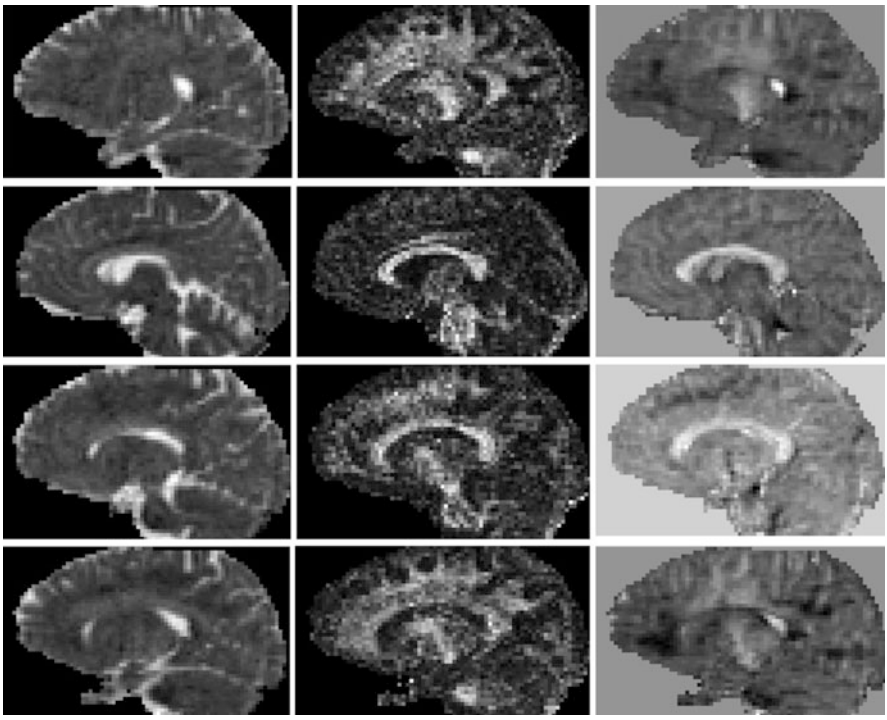

Fig. 7 Sagittal view of the results on real data: (*left column*) MD map, (*middle column*) FA map, and (*right column*) proposed diffusion map (DM)

provide information, which is present in both mean diffusivity (MD) and fractional anisotropy (FA) maps, as conventionally employed as quantitative maps in human brain. The exact mathematical relationship between DM and FA, MD along with the clinical applications of the proposed quantitative map will further be investigated in our future works.

References

1. Basser, P.J., Mattiello, J., LeBihan, D.: MR diffusion tensor spectroscopy and imaging. J. Biophys. **66**(1), 259–267 (1994). doi:10.1016/s0006-3495(94)80775-1
2. Mori, S., Zhang, J.: Principles of diffusion tensor imaging and its applications to basic neuroscience research. Neuron **51**(5), 527–539 (2006)
3. van der Maaten, L.J., Postma, E.O., van den Herik, H.J.: Dimensionality reduction: a comparative review. J. Mach. Learn. Res. 10(1–41), 66–71 (2009)
4. Schölkopf, B., Smola, A., Müller, K.-R.: Nonlinear component analysis as a kernel eigenvalue problem. Neural Comput. **10**(5), 1299–1319 (1998)
5. Tenenbaum, J.B., De Silva, V., Langford, J.C.: A global geometric framework for nonlinear dimensionality reduction. Science **290**(5500), 2319–2323 (2000)

6. Coifman, R.R., Lafon, S.: Diffusion maps. Appl. Comput. Harmon. Anal. **21**(1), 5–30 (2006)
7. Hamarneh, G., McIntosh, C., Drew, M.S.: Perception-based visualization of manifold-valued medical images using distance-preserving dimensionality reduction. IEEE Trans. Med. Imaging **30**(7), 1314–1327 (2011)
8. Khurd, P., Baloch, S., Gur, R., Davatzikos, C., Verma, R.: Manifold learning techniques in image analysis of high-dimensional diffusion tensor magnetic resonance images. Paper Presented at the IEEE Conference on Computer Vision and Pattern Recognition, 2007 (CVPR'07), pp. 1–7 (2007)
9. Goldberg, Y., Zakai, A., Kushnir, D., Ritov, Y.A.: Manifold learning: the price of normalization. J. Mach. Learn. Res. **9**, 1909–1939 (2008)
10. Nadler, B., Lafon, S., Coifman, R., Kevrekidis, I.G.: Diffusion Maps-A Probabilistic Interpretation for Spectral Embedding and Clustering Algorithms Principal Manifolds for Data Visualization and Dimension Reduction, pp. 238–260. Springer, New York (2008)
11. Nadler, B., Lafon, S., Coifman, R.R., Kevrekidis, I.G.: Diffusion maps, spectral clustering and reaction coordinates of dynamical systems. Appl. Comput. Harmon. Anal. **21**(1), 113–127 (2006)
12. Farup, I., Hardeberg, J.Y., Bakke, A.M., Kopperud, S., Rindal, A.: Visualization and interactive manipulation of color gamuts. Paper presented at the Color and Imaging Conference (2002)
13. Leemans, A., Jeurissen, B., Sijbers, J., Jones, D.: ExploreDTI: a graphical toolbox for processing, analyzing, and visualizing diffusion MR data. Paper Presented at the 17th Annual Meeting of International Society of Magnetic Resonance in Medicine, p. 3537 (2009)